Master's Thesis

Retrosimulation of a Space Traveling-Wave Tube 250 W, Ka-band, 4-stages collector

Dorian Bugnot

Department of Electrical and Information Technology,
Faculty of Engineering, LTH, Lund University, November 2015.

Thales Electron Devices
Vélizy, France

Lunds universitet
Lunds Tekniska Högskola

THALES

Master Thesis
Engineering Physics - High-Frequency and Nanoelectronics

Retrosimulation of a Space Traveling-Wave Tube 250 W, Ka-band, 4-stages collector

Dorian Bugnot

Company Supervisors : *Pierre Lecuyer*
Jean Gastaud
LTH Examinator : *Lars – Erik Wernersson*

January 13 - July 11, 2014

Acknowledgements

First and foremost, I would like to thank to my supervisors, Mr Pierre Lecuyer and Mr Jean Gastaud for the valuable guidance and advice. They inspired me greatly to work in this project and they were abundantly helpful and offered invaluable assistance and support.

Besides, I wish to express my sincere gratitude to Jean-François David and Pierre Bernardi who always provided me support and guidance when I was facing problems with computer codes. I would also like to convey thanks to my office colleagues, Alexandre Perdereau, Fabrice Vasseur and Marc Lefèvre, for giving me relevant advices every time I asked them and for receiving me extremely favourably. I would like to thank Telma Pereira and Pascal Taphanel for the time they offered me for practical explanations and measurements.

I would like to show my greatest appreciation to Alain Laurent, which made this project possible, and the experts, Frédéric André and Alain Durand for their tremendous advices. My special thanks to Philippe Thouvenin for his support and confidence.

Abstract

The internship is dedicated to the modeling of RF and electrical performances of a 250 W Ka traveling-wave tube, using computation codes developed internally. The objective was to compare simulations and measurements in order to design a 5-stages collector.

The modeling of the interaction wave -beam (RF model) is discussed in the first part. Simulations are done with the internal code MVTRAD. In particular, the gain (at saturation and small signal), the output power and the phase shift are simulated and compared to measurements. Then, we model the collector with the internal code COLLECTD. We look at the electron trajectories and velocities in the collector and we compare the current collected on each electrode to the measurement.

Discrepancies have been found between simulations and measurements so that the codes have not been found reliable enough for creating a new design. The objective of the internship changed and we focused on understanding the collector simulation discrepancies.

Acronyms

TWT	:	$Traveling - Wave\,Tube$
VS	:	$Velocity\,Spectrum$
MDC	:	$Multistage\,Depressed\,Collector$
$MVTRAD$	:	$MouVemenTs\,RADiaux$
PPM	:	$Periodic\,Permanent\,Magnets$
$VSWR$	:	$Voltage\,Standing\,Wave\,Ratio$
BSE	:	$Back - Scattered\,Electron$
SE	:	$Secondary\,Electron$
V_H	:	$Helix\,Voltage,\,it\,is\,equal\,to\,the\,Anode\,Voltage\,by\,definition$

Contents

Introduction

In satellite systems, on-board repeaters shall deliver always more RF power. Specifically in Ka-Band applications like HDTV or Internet, the satellite Capacity must be increased to improve the Data Rate Transfer. This Capacity increase leads to a substantial increase of Specified RF Output Power. Besides, a high electric efficiency is required for space applications because the electric payload power has to be minimized.
Nowadays the payload is typically about 10 kW and the space Traveling-Wave Tubes delivers 130 W, therefore increasing the electric efficiency by 2 points percentage (rising from 63% to 65%) would represent a power payload decrease of 300 W. The way of increasing the electric efficiency lies in the adding of a collector stage. The collector is a considerable mainstream development for space TWTs. High power TWTs with a increased efficiency are nowadays essential to keep on leading the market of the Ka-Band.

The internship takes place in a delicate context insofar as new results are expected by the development department for a while. The internship focuses on a 250 W space TWT operating in Ka-Band. The objective is to fit a 4-stages collector by simulation in order to define a new collector design resulting in a better electric efficiency. The internship is divided in two parts, the fit of the collector at first and then the optimization of the design.
After describing the sub-assemblies of the TWT layout and I present the basics of the TWT theory. Then, we will introduce the Thales simulation codes and show the simulation fit of the TWT. In the end of the report, we will focus on the issues related to the simulation and the possible means to solve them. A major problem for the collector simulation, related to the electron beam velocity, is highlighted in this report. I propose means to understand and quantify the problem. Some have already been implemented.

Chapter 1

Traveling-Wave Tube Theory

1.1 Overview

A TWT (Figure 1.1) is a high power amplifier which can deliver more than several hundreds of Watt and operating in the RF range 1 GHz - 300 GHz. The spectrum is divided in bands, and in space communications the band reference is usually the downlink band, i.e. the band used to communicate from the satellite to the ground. There can be an offset of several GHz between the uplink and the downlink band. Here are some typical bands for space applications:

X Band : 8 - 12 GHz. Military and meteorological applications. Short communications range due to water absorption.

Ku Band : 10.75 - 12.75 GHz.

Ka Band : 17.3 - 21.2 GHz. Civil & Military applications, Satellite Internet & TV access.

Q Band : 37.5 - 42.5 GHz. Band dedicated to control the satellite to free the full operating bandwidth for data transfer.

Space TWT are designed to deliver commonly between 50 W and 250 W. The tube consists of three main sub-assemblies :

an electron gun : The function of the electron gun is to produce electron by thermionic-emission and accelerate them into the delay line.

a delay-line : The function of the delay line is to amplify the wave, the electron beam giving its kinetic energy to the wave circulating on the helix around it.

a collector : The function of the collector is to collect the different electron energy in order to minimize the thermal dissipation of the TWT.

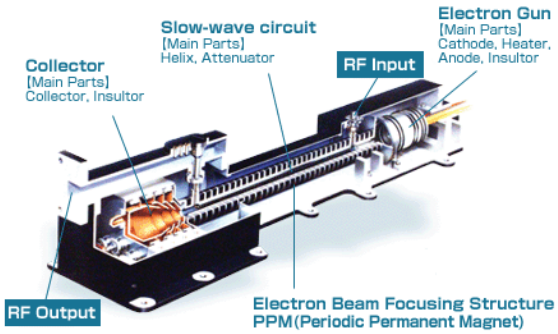

Figure 1.1: Schematic of an Traveling-Wave Tube.
(From Nec Network and Sensor Systems website :
http://www.netcomsec.co.jp/en/english/products/twt/index.html)

1.1.1 Electron Gun

It consists of a heated up cathode which produce the electrons and a system with the Anode and the Wenhelt Electrode to focus them. The anode creates an accelerating field which drives the electrons from the cathode into the delay line (Figure 1.2). Additional constraints are coming from the cathode technology that limits the current density at its surface to $2.5A/cm^2$ for 15 years operation.

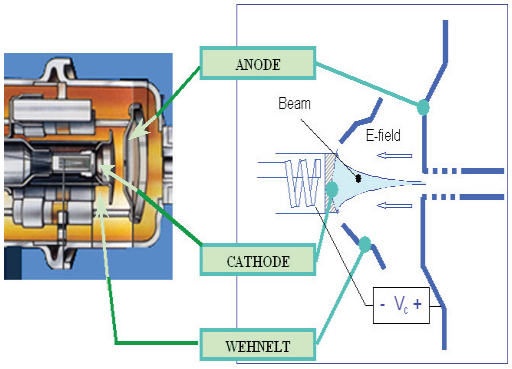

Figure 1.2: Schematic of a Cathode.
(From Thales Internal C. Chastang Master Thesis Report, "Optimisation de l'optique électronique du Tube à Ondes Progressives 170W en bande Ka pour applications spatiales", 2009)

1.1.2 Delay Line

The delay line is the structure where the amplification takes place. It is a slow-wave circuit where the RF wave travels on the helix at approximately the same speed as the electron beam. The electron beam

flows at the center of the helix as shown in Figure 1.3. The interaction with the beam is continuous, that is, the electron beam gives its kinetic energy to the wave circulating around it all along the delay line [1].
The helix is hold by three support rods in the body (barrel), and the beam is focused with permanent periodic magnets (PPM).

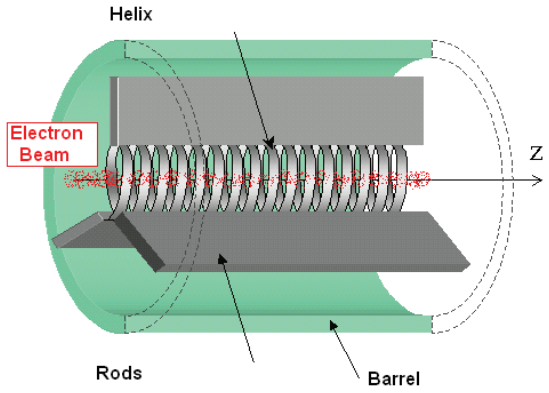

Figure 1.3: Schematic of the helix hold by the three rods inside the barrel.

Permanent Periodic Magnets (PPM) focusing

The beam flows in the middle of the helix on a relatively long distance (about 15 cm) and is kept focused thanks to the magnetic field. We try to to have the minimum possible beam interception (the best possible focusing) and the best possible laminarity (no crossing of trajectories). The ligthest way of creating such magnetic field is to use PPM (Figure 1.4) [2, 3].

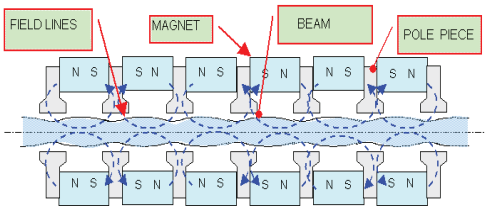

Figure 1.4: Effect of the PPM focusing on the beam.
(From Thales Internal C. Chastang Master Thesis Report, "Optimisation de l'optique électronique du Tube à Ondes Progressives 170W en bande Ka pour applications spatiales", 2009)

Dielectric Support Rod

The helix is held by three dieletric rods which provide:

- mechanical strength
- thermal dissipation
- accurate control of the gain

1.1.3 Collector - Multistage Depressed Collector (MDC)

The function of the collector is to collect the electrons. Once injected in the collector, the electrons trajectories are ruled by the Lorentz Force $\vec{F} = q\vec{E} + q\vec{v} \wedge \vec{B}$ (i.e. the electrostatic and magnetic field in the collector) and the space charge of the beam (force produced by the electrons on each other). With a collector at the same potential than the body of the tube, electrons strike the collector at relatively high velocity. Electron energy is converted to heat at the surface of the electrode. By reducing (depressing) the voltage on the collector below the body potential, the velocities of the electron striking the collector and the heat generated in the collector are reduced. As a result, the collector recovers some of the power in the spent electron beam (beam leaving the RF circuit). Nowawadays, collector are made up of four electrodes with depressed potential, thus we call it Multistage Depressed Collector (MDC) (to be discussed in further detail in section 2.2.2).

1.2 A deeper look

1.2.1 Interaction principle: from Kinetic to Potential Energy

In Figure 1.5, the wave and the beam are propagated in the same direction (z) at about the same speed so the electrons experience a continual force toward region (A). As a result, an electron bunch starts to form in region (A). The field produced by the bunching electrons in the beam causes electrons on the helix to move away from the region adjacent to (A) toward the (B) regions. Thus, the field produced by the helix is enhanced, and this, in turn, increases the bunching of the beam.
To produce growth of the field in the circuit, energy is extracted from the electrons. Thus, the velocity of the circuit field must be slightly less than the electron velocity so that the electron bunches move into the decelerating field region [4]. The mutual interaction of the beam and circuit result in an exponential growth of the signal level.

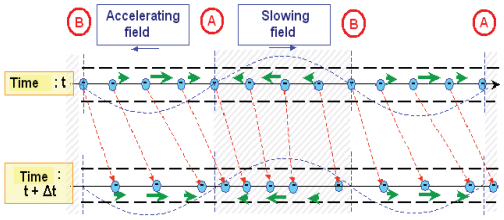

Figure 1.5: Illustration of the interaction principle and electron bunching in a helix TWT. (From J. Plouin, "Injection d'harmonique dans un Tube à Ondes Progressives : amélioration de la puissance de sortie". Condensed Matter. Ecole Polytechnique X, 2004. French. <tel-00007146>)

1.2.2 Velocity Spectrum & MDC

As a result of the bunching process, the electrons, all sent with the same axial speed, end up at the RF output with a wide range of speed. That depends obviously of the interaction intensity : the bigger the interaction, the more scattered the velocity [5]. For convenience, the electron velocity is expressed in Volt [V], derived in the following equations:

$$V = (\gamma - 1).\frac{c^2}{\frac{e}{m_0}}$$

V : *electron velocity [V]*
γ : *the Lorentz factor*
c : *speed of light*
e : *charge of the electron*
m_0 : *mass of the electron*

$$\gamma = \frac{1}{\sqrt{1 - (\frac{v_z}{c})^2 - (\frac{v_r}{c})^2 - (\frac{v_\theta}{c})^2}}$$

v_z : *axial velocity*
v_r : *radial velocity*
v_θ : *azimutal velocity*

As an example in Figure 1.6, we represent the cumulative current versus the speed in Volts. Electrons are sent at potential V_H (blue dashed line) under strong interaction (saturation) and the estimated velocity spread from V_{min} to V_{max}. For instance, it means that around 85% of electrons has been slowed down and that 15% of electrons has been accelerated. In this diagram the surface are powers:

1. The thermal dissipation is the dashed area under the curve. A variation of cumulative current in a small intervalle $[V_i, V_{i+1}]$ is $\frac{dI}{dV}$, thus the thermal dissipation is given by:

$$\begin{aligned} \int_i^{i+1}(V - V_i)\frac{dI}{dV}\,dV &= ((V - V_i).I)_i^{i+1} - \int_i^{i+1}\frac{dI}{dV}\,dV \;\; (integrationByParts) \\ &= (V_{i+1} - V_i) * I_{i+1} - \int_i^{i+1}\frac{dI}{dV}\,dV \end{aligned}$$

   Thus, in terms of area between two points i and i+1 :

   Thermal Dissipation = Area under the Curve - Blue Area = Pink Area

   Between V_{max} and VC it is then the dashed area.

2. The electric power is the yellow box area (the electrode catches electrons so the power supply supplies current):

$$CollectorElectricPower = \Sigma\,(V_H - V_{C_i}).I_{C_i} = (V_H - V_C).I_C \;\; (only\,1\,stage\;here)$$

   We add the power of the filament $V_F.I_F$ and the power of the helix $V_H.I_H$ when considering Consumption (WT).

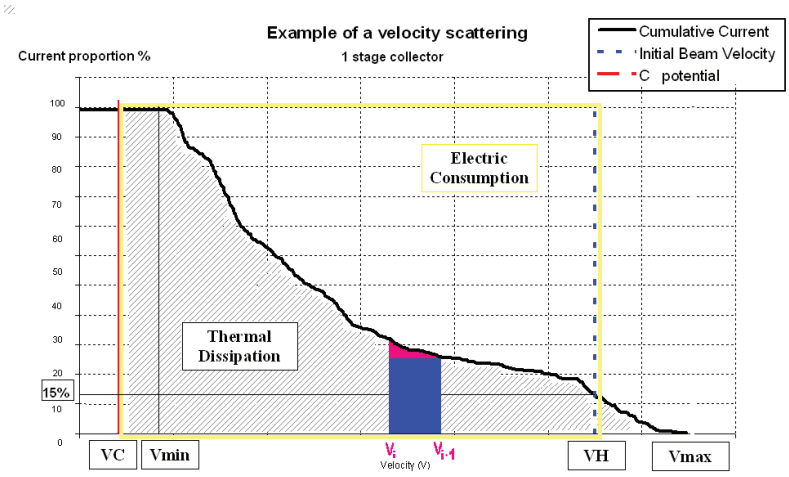

Figure 1.6: Spectrum velocity [in Volts] of an electron beam at the RF output at saturation. Thermal dissipation (dashed area) and electric power (yellow box) for a 1 stage collector.

Ideal Collector

An ideal collector would collect each electron on an electrode which has the lowest potential the electron can reach. So, the ideal collector would have as many electrodes as electron velocities. That can be explained with hands: to catch a ball rolling down a hill without being struck, you would better catch it on the other side of the hill at the same height (assumed no loss). It is the same explanation for electrons, the bigger the voltage between the electron and the electrode, the bigger the thermal dissipation (Figure 1.7).

Multistage Depressed Collector (MDC)

As said in section 2.1.3, collectors have nowadays four electrodes with depressed potentials to recover some of the power of the spent beam and to minimize the thermal dissipation and the electric power. In Figure 1.6, the objective is to reduce the areas as much as possible. As seen in Figure 1.8, with four stages, the yellow area and dashed area are considerably decreased, the four stage collector decreases both the thermal dissipation and the electric consumption of the collector. The velocity spectrum is essential to understand and to predict the current distribution and the thermal dissipation of the collector. Though, the prediction is made under the assumption that the electrons are collected on the electrodes which corresponds to their speed, i.e. the electrode having a potential just smaller than the electron velocity. To simplify, fast electrons are collected on high potential electrodes and slow electrons on low potential electrodes. In reality this is not completely true, a fast electron can be collected on a low potential electrode due to secondary emission. It is a critical issue for collectors and for the TWT. Secondary emission theory is developed in the next section.

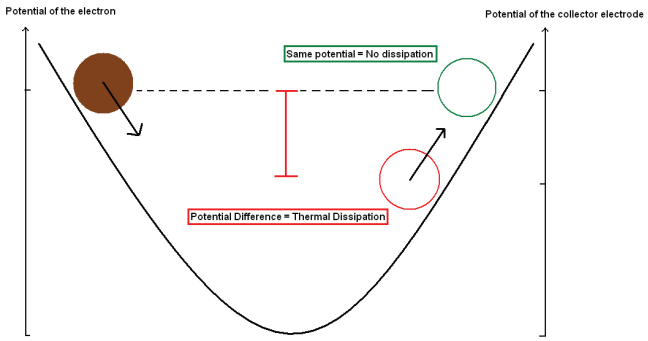

Figure 1.7: Thermal dissipation due the potential difference between the electron velocity and the electrode potential.

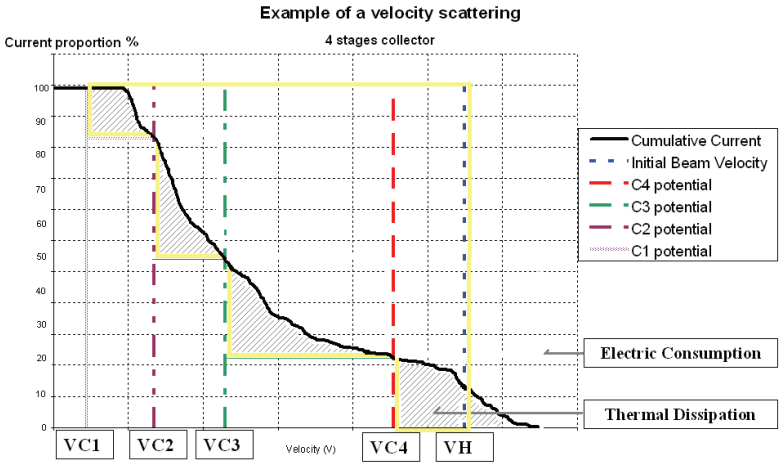

Figure 1.8: Spectrum velocity [in Volts] of an electron beam at the RF output at saturation. Thermal dissipation (dashed area) and electric power (yellow box) for a 4 stage collector.

1.2.3 Electron Emission in the collector

Modern multistage depressed collectors (MDC's) for microwave tubes provide (by design) electrostatic suppression of low-energy, secondary-electron emission generated on most of the electrode surfaces which receive incident current. Nevertheless, some backstreaming of secondary electrons is always present. This is due to energetic secondaries, actually elastically and inelastically scattered primaries (Figure 1.9), and the presence of some incident current on regions of the electrodes where no suppression occurs [6]. Such back-streaming results in degradations of the overall tube and collector efficiencies.

Three types of secondary electrons are distinguished :

Back-Scaterred Electron - elastic (no energy loss) or inelastic (energy loss) scattering. The BSE coefficient does not depend on the incident energy W_{inc} but depends on the incident angle α:

$$\eta(\alpha) = (1 + cos(\alpha))^{\frac{-9}{\sqrt{Z}}}$$

α : *incident angle*
Z : *atomic number of the material*

(True) Secondary Electron - inelastic scattering, electrons are reemitted with less 50 eV. The SE coefficient δ depends on the incident angle and the incident energy:

$$\delta = \frac{\delta(0)}{cos(\alpha)}$$

$\delta(0)$: *the dependence on* W_{inc} *is shown in Figure 1.10*

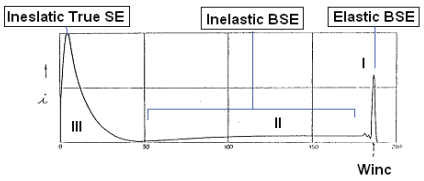

Figure 1.9: Energy spectrum of secondary electron: Elastic Back-Scattered Electron (I), Inelastic Back-Scattered Electron (II), True Secondary Electron (III).
(H. Seiler, Secondary electron emission in the scaning microscope, J. Appl. Phys., 54(11) (1983))

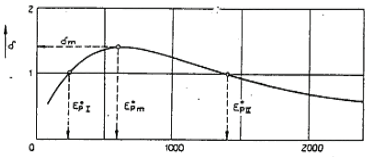

Figure 1.10: Secondary electron coefficient versus the incident energy.
(H. Seiler, Secondary electron emission in the scaning microscope, J. Appl. Phys., 54(11) (1983))

In the case of the energetic, elastically and inelastically scattered primary electrons, the electrostatic suppression is much less effective and a greater probability exists of secondary-electrons backstreaming to less depressed MDC stages or to the TWT body itself (Figure 1.11). All such backstreaming of secondary electrons results in:

1. a reduction of the spent beam power recovered by the collector
2. a reduced TWT overall and collector efficiencies

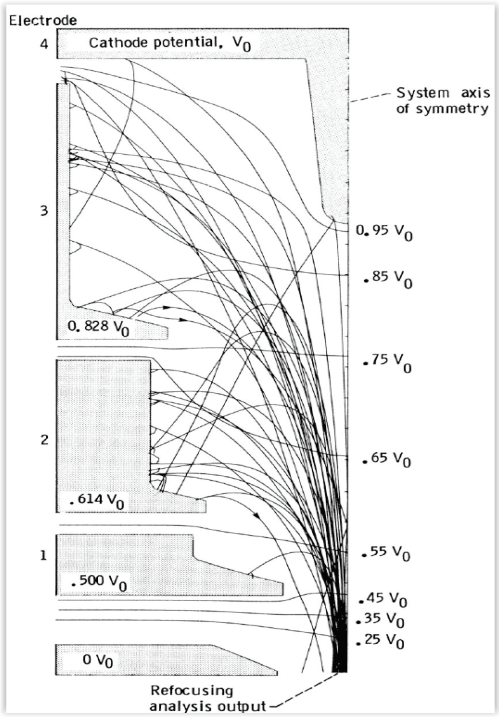

Figure 1.11: Charge trajectories for incident primaries and low energy (true) secondary in a four-stage depressed collector, TWT operating at saturation.
(A.S. Gilmour, Microwave Tubes, Figure 12.8, p.334, originally from H.G. Kosmahl, Proc. IEEE, 1982)

1.3 Space TWT Figure of Merits

For a frequency in the bandwidth, three figure of merits are defined, the beam efficiency, the collector efficiency and the overall efficiency [7].

1.3.1 Transfer Curve of the amplifier

An easy way to describe gain and saturation in a TWT is to plot the output power versus the input power as shown in Figure Figure 1.12. The two important region are the small signal and the saturation regions. At small signal levels, a change the output power is proportional to a change input power, so that the gain is constant. At saturation, the gain decreases and the the operation becomes non-linear. TWT users often use the term B̈ack-Off ;̈ this refers to linear region. For example, setting the input power at 20 dB (input) back-off means we set the input power 20 dB less than the input power for which the TWT saturates. As we are under saturation, we are in linear / small signal region.

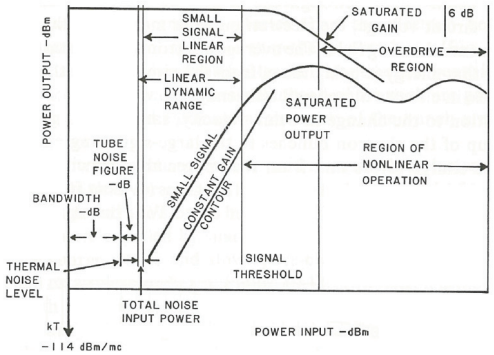

Figure 1.12: Dyanamic Characteristics of a TWT : Output Power versus Input Power.
(A.S. Gilmour, Microwave Tubes, Figure 10.17, p.258, originally from Huges Aircraft Co., TWT and TWTA Handbook)

1.3.2 Preliminar Definitions

Consumption (WT)

It is the Electric Consumption (WT) defined as the sum of the electric power of all the collector electrodes (WCi), the helix (WH) and the filament (WF) ; with $W_x = V_x.I_x$.
Assuming the case of a 4-stages collector:

$$WT = WC_1 + WC_2 + WC_3 + WC_4 + W_H + W_F$$

RF losses

The RF losses along the helix is a percentage of the RF power (P_{out}).

Helix Power & Correction Coefficient

$$WH = I_H.V_H.(1 - 2\eta_{int})$$

η_{int} *: beam efficiency.*

The helix power due to electron interception on the helix is corrected by a factor $I_H.V_H.(1 - 2\eta_{int})$ because all electrons that strike the helix do not have the speed V_H. In particular, some are slower due to the interaction with the wave which has slowed them down.

1.3.3 Beam efficiency

It represents the efficiency of the interaction: How much power can we get from a beam ?

$$Beam\,Efficiency = \frac{Output\,Power}{Beam\,Power} = \frac{Output\,Power}{V_H.I_K}$$

1.3.4 Collector Efficiency

The collector efficiency reflects the capacity of the collector to recover power from the spent beam. All the power not recovered is dissipated. So a good collector dissipate as less as possible (small area in section 2.2.2). The collector dissipation and collector electric consumption are improved with the MDC [8].

$$Injected\,Power = V_H.I_K - P_{OUT} - RF\,losses - I_H.V_H.(1 - 2\eta_{int})$$

$$Actual\,Collector\,Dissipation = WT - P_{OUT} - RF\,losses - I_H.V_H.(1 - 2\eta_{int}) - V_F.I_F$$

We compare the injected power in the collector (spent beam power) to the collector dissipation.

$$Collector\,Efficiency = 1 - \frac{Actual\,Collector\,Dissipation}{Injected\,Power}$$

1.3.5 Overall & Cross Efficiency

The overall efficiency - implied electric efficiency - is the most important figure of the TWT. As a reminder, the objective of the internship is to increase the overall efficiency.

$$Overall\,Efficiency = \frac{Output\,Power}{Electric\,Consumption\,(WT)} = \frac{Output\,Power}{WC_1 + WC_2 + WC_3 + WC_4 + W_H + W_F}$$

To get an efficiency through the whole bandwith, we define a **cross efficiency** as the ratio of the average Output Power in the bandwidth over the maximum Consumption in the bandwidth:

$$Cross\,Efficiency = \frac{P_{OUTmin}}{WT_{average}}$$

Chapter 2

Fitting Simulations

So far, we have observed the tube from a theoretical point of view. After setting the context and the customer need (Introduction & Chapter 1), we have described the physics which governs a TWT (Chapter 2). Now, we will focus on the tube performances and the simulation with the aim of improving the performances.

2.1 Simulation Codes (MVTRAD & Collect3D)

Home-made codes and CAE sofware are used to modelize the TWT. The delay line is simulated with MVTRAD, the collector is simulated with COLLECT3D. In Figure 2.1, the simulation map is described to get a global understanding of the simulation organization.

2.1.1 MVTRAD - Helix Simulation

MVTRAD is a 2.5D Particle-In-Cell (PIC) code meant for the simulation of the wave-beam interaction in helix TWTs [9]. It was developed to get an estimation of the electronic velocity spectrum at the RF output (also the collector input), with the aim of refining the MDC simulation. MVTRAD needs four data types and estimates the interaction and the velocity spectrum of the electron beam, as shown in the top of Figure 2.1. ELF2D, another Thales code, is used to compute the magnetic field in the delay line.

2.1.2 COLLECT3D - Collector Simulation

Collect3D is meant for the 3D modelisation of electron beam in MDC with consideration of secondary emission: primary, true secondary, elastic and inelastic back-scattered electrons. It is based on a 3D PIC code on which a secondary emission model has been added. The 3D aspect is necessary when the collector geometry and/or the magnetic field are not axisymmetric. Thanks to MVTRAD, the beam can be modulated by the RF wave before entering into the collector. In addition to the particle injection file from MVTRAD, COLLECT3D needs a collector mesh file, a magnetic field and the definition of the electrode potentials (bottom of Figure 2.1). The code computes the electron position and velocity step by step until the electron strikes the electrode. Then, we get the current distribution

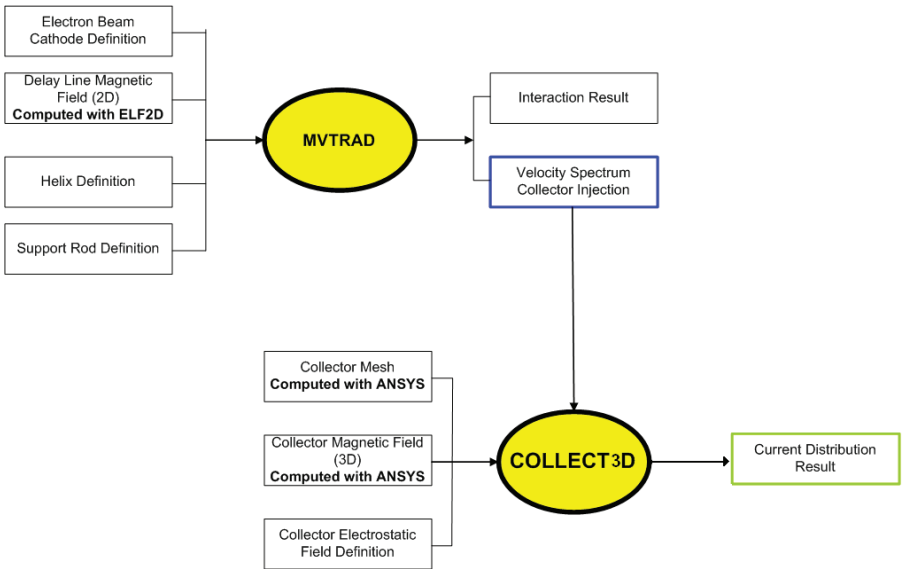

Figure 2.1: MVTRAD & COLLECT3D Execution Environment.

on the electrodes and an estimation of the thermal dissipation. Moreover, the computed electron paths are observable with an interactive interface INTERF3D.

Preliminar Computations with ANSYS

The 3D magnetic field in the collector and the collector mesh are computed with the commercial CAE software ANSYS. Two screenshots are presented in Figure 2.2. It should be noticed that the electromagnetic field is to be analyzed, therefore the vacuum inside the collector is meshed (and not the collector bulk).

Visualization of the Electron Trajectories - INTERF3D

After computation, the electron trajectories can be seen with INTERF3D (Figure 2.3), an interactive interface which has been developed together with COLLECT3D. Therefore, we can:

- see the path of each electron trajectory from the input collector to the electrode impact point
- see the nature of the electron (primary, true secondary, back-scattered)
- sort out the electrons by input energy
- sort out the electrons as a function of the electrodes

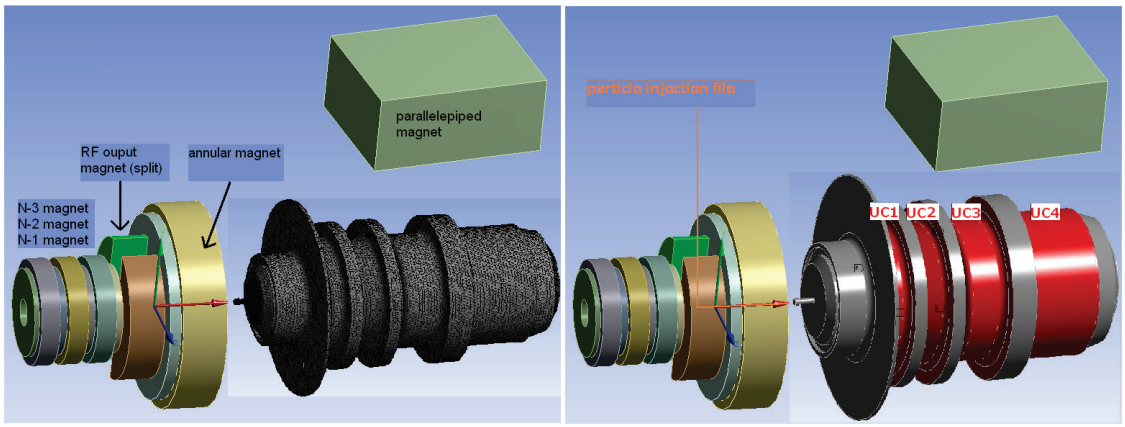

Figure 2.2: Exemple of screen shot of ANSYS.

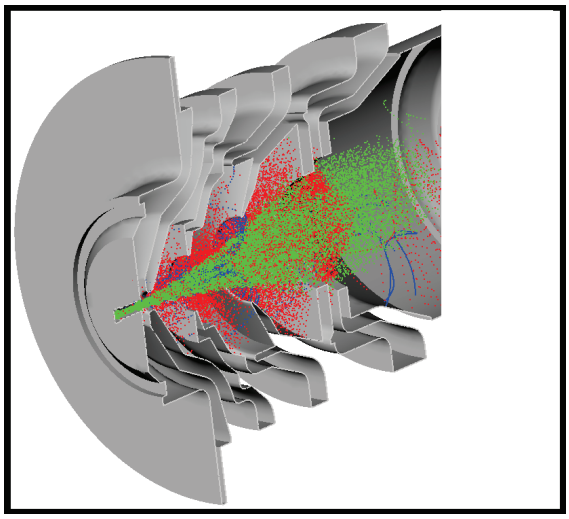

Figure 2.3: Example of screen shot of Interf3D. The green particles are primaries, red are back-scattered and blue are secondaries.

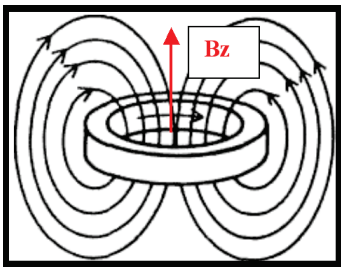

Figure 2.4: Repesentation of the field lines of an annular magnet. We measure the axial field Bz.

2.2 Simulation Results

Even if we are only interested in the velocity spectrum for collector simulation, we fit the electric performances of the TWT (interaction result box in Figure 2.1). First, the beam properties are not measurable (so no fit possible), and a good fit of the electric performances means a good modelization of the interaction so certainly a good velocity spectrum.

2.2.1 RF Electric Performances Fit (MVTRAD)

The input data of the delay line are measured as accurately as possible. The value of each magnet has to be measured separately. As they are annular, we measure the field on the axe Bz shown in Figure 2.4.

Then, the overall magnetic field created by all the permanent periodic magnets is computed with ELF2D, a 2D numeric simulation home made code. Although, all precautions are taken regarding the input simulation parameters, there is always a discrepancy between the simulation and the measurements.

RF Electric Performances Characteristics

After selecting the solution which gives the best MGV fit, we compute the output figures of the TWT. We plot the gain at saturation in Figure 2.7, the output power at saturation in Figure 2.5 and the interaction efficiency at saturation in Figure 2.6. Finally, we plot the gain in small signal in the bandwidth (Figure 2.8) and the phase shift between saturation and small signal (Figure 2.9). Indeed, the phase of the wave is the same for all frequencies at small signal, however, at saturation the phase takes different values. The phase is somehow related to the interaction (non linear phenomenum) and the stronger the interaction, the more the phase drifts. As the interaction is more efficient at high frequency, the phase shift is bigger at the maximum operating frequency. It is a limiting factor and the specification usually requires a **Phase Shift** < 45.

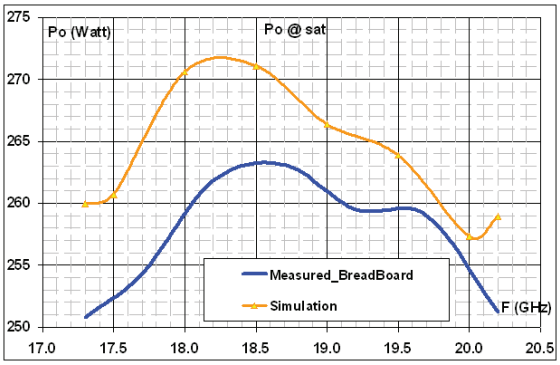

Figure 2.5: Comparaison of simulated and measured Output Power @ saturation in the band.

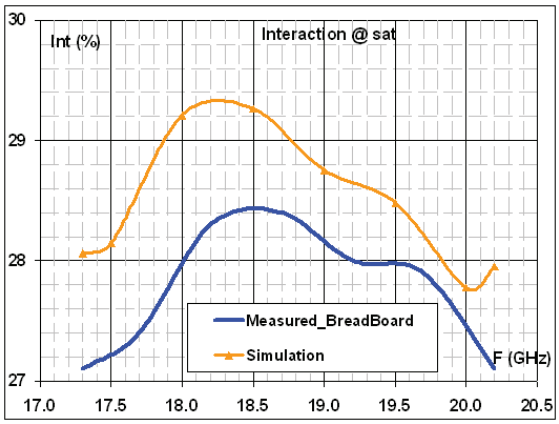

Figure 2.6: Comparaison of simulated and measured Interaction Efficiency @ saturation in the band.

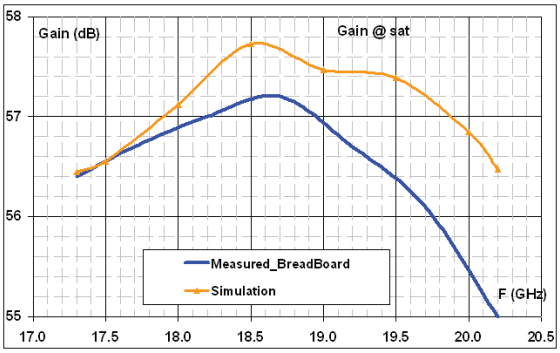

Figure 2.7: Comparaison of simulated and measured Gain @ saturation in the band.

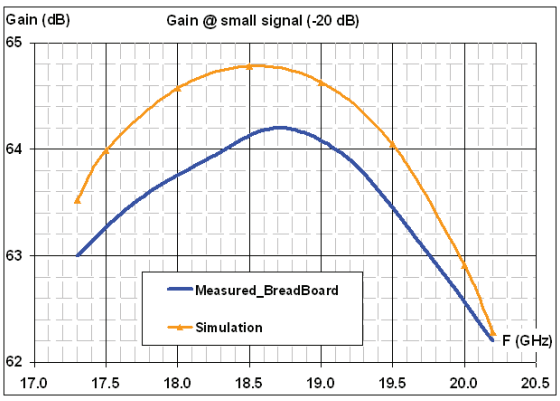

Figure 2.8: Comparaison of simulated and measured Gain @ small signal in the band.

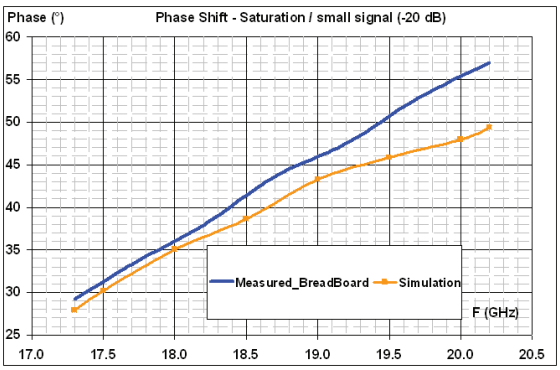

Figure 2.9: Comparaison of simulated and measured Phase Shift in the band.

The simulation curves fit pretty well the measurements of the RF electric performances. We get less than 4% disprecancy on the Output Power and and less than 2 % on the Gain. The Voltage Standing Wave Ratio (VSWR) is not taken into account in the simulation, then we correct the simulated Output Power with a measured VSWR after the simulation. However, the simulation is still optimistic and all the output characteristics but the phase shift are slightly overestimated. To sum up, by adjusting the dielectric permittivity, the attenuation and the tightening of the rod we get a good fit of the characteristics of the delay line. Actually, those output parameters are not crucial for the collector fitting, what is really at stake is the shape of the electron beam at the RF output, but it is, unfortunately, not measureable. Then, getting a good fit of the electric performances of the delay-line is the best way to get the best approximated beam shape.

2.2.2 Current Distribution and Thermal Dissipation Fits (COLLECT3D)

In Figure 2.10, the current distribution on the four electrodes (IC_1, IC_2, IC_3, IC_4 - four plots) are compared to the measurement from strong back-off up to close to saturation.

First Comments

The shape of the curves are well fitted for the four stages. IC1 does not seem that good but the scale of the y-axis (the current) is small. That is a first satisfaction and that validates our physical and mathematical models.

- **IC4 is decreasing :** when the normalized input power ($P_{in} - P_{inSAT}$) increases, i.e. when we get closer to the saturation, there is more interaction. As a result, the electrons loose more and more kinetic energy, they become slower. Thus, less and less electrons have enough velocity to enter in the fourth stage, IC4 decreases.
- **From -17dB to -9dB :**As electrons do not have enough energy to pass the C4 barrier, they are striking C3. IC3 increases and IC4 decreases, they exchange the electrons.
- **From -9dB to -1dB :** IC3 decreases in turn for the same reason that IC4 decreased, with the increasing interaction, electrons do not have enough energy to pass the C3 barrier. They are collected on C2 ; indeed, IC2 is increasing.
- **All electrons** always have enough energy to pass the C1 barrier. The first stage is a protection against the backward current (from the collector to the delay line) which can cause oscillations. The backward current can come from primary electrons which are not able to pass the C2 barrier, but it can also be due to secondary and back-scattered electrons.

Comments about the simulation

As said in the first place, the tendency of the curves are pretty well fitted. There is a discrepancy between the simulation and the measurements though. This is obvious in particular for IC4 and IC3. The simulated IC4 is around 10 mA less than the measurements and 15 mA in the worst case. On the opposite, simulated IC3 is always bigger than the measurement by around 10 to 15 mA. It gets better when approaching the saturation. Anyway, we have now an issue to deal with, why are the electrons not collected enough on C4 ? Why is IC3 such big at -9 dB back-off ?

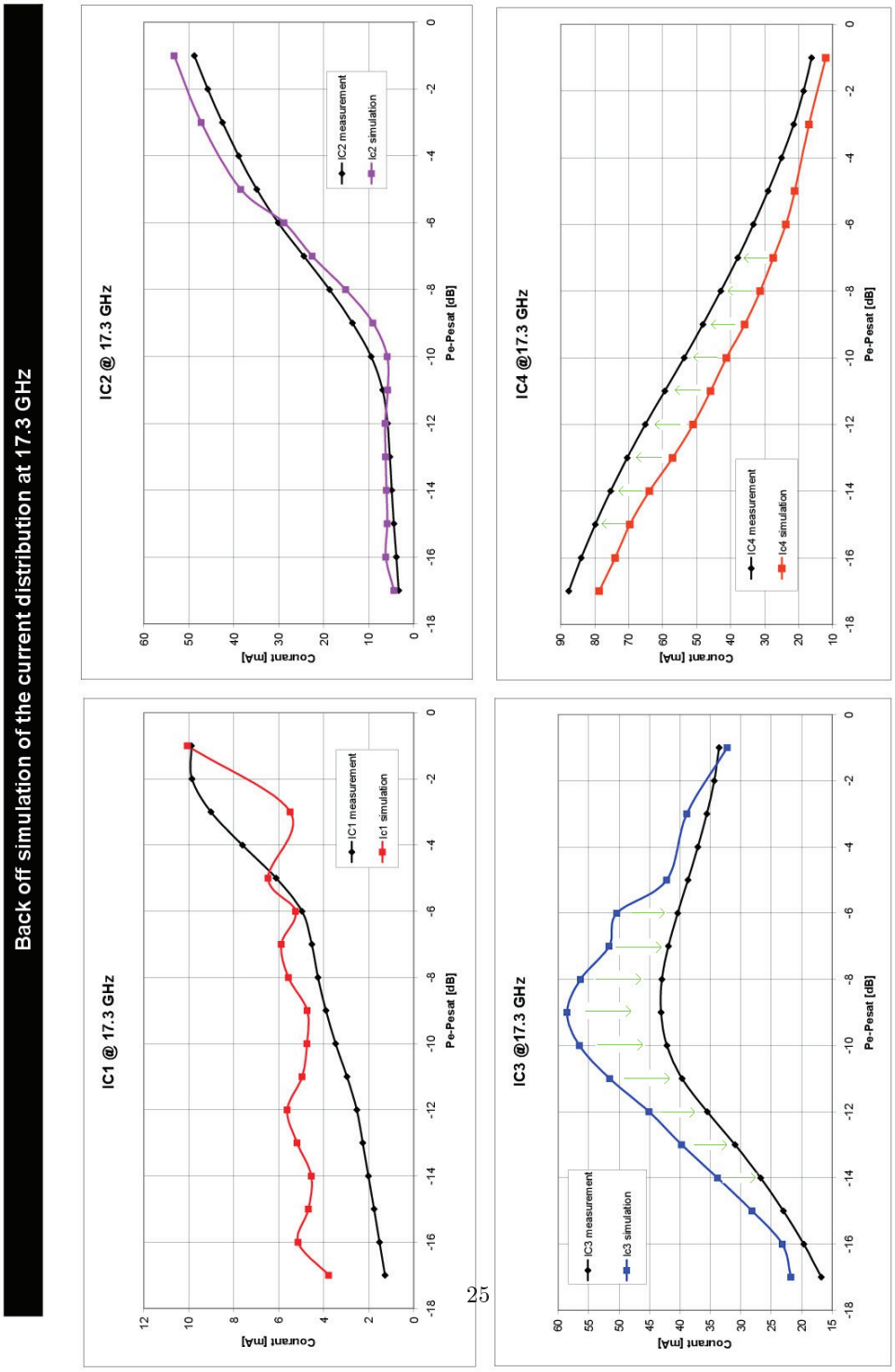

Figure 2.10: Collect3D Simulation result - Current Distribution.

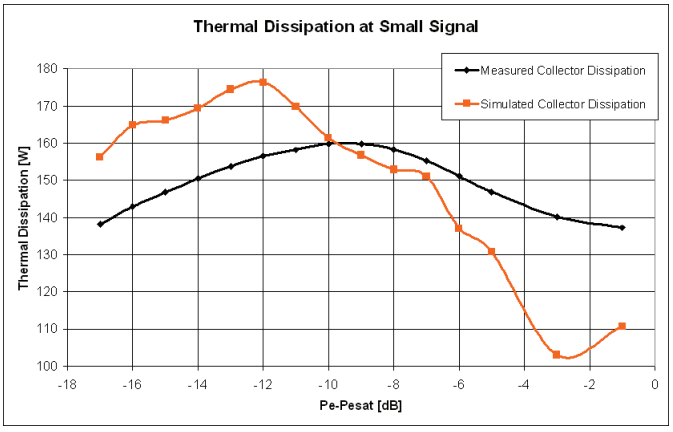

Figure 2.11: Collect3D Simulation result - Thermal Dissipation.

Thermal Collector Dissipation Fit

As shown in the measurement in (Figure 2.11), the maximal thermal dissipation of the collector is reached at back-off 9 dB. The thermal critical design parameter is set regarding the maximal dissipation which takes place in back-off, this is why the simulation in back-off is crucial. To sum up, the RF electric performances of the helix (gain, output power) are design factors at saturation and the thermal collector dissipation is a design factor in back-off.
Even before plotting the simulated thermal dissipation (Figure 2.11), we could guess that it is not going to be a perfect fit because of the discrepancy in the current distribution. Indeed, the current and the thermal dissipation are closely related. Intuitively, the bigger the voltage between the electron and the electrode, the bigger the thermal dissipation of the electron (see Figure 1.7).

So far, we have fitted with success the RF electric performances of the delay line with MVTRAD. We have injected the result of this computation in the collector, and the result shows some discrepancy with the measurements. The next step is to understand why there is such a low simulated IC4 current. If we solve this issue, the other currents should get better - at least IC3 - as we saw earlier in this section that IC3 and IC4 are going hand by hand.

Synthesis of the overall electric parameters fit

The comparison of the electric parameters of the TWT shows that in spite of a good fit of the RF electric performances of the helix, we get a bad collector fit which results in a bad fit of the overall TWT electric performances.

Chapter 3

The Root Cause - Velocity Spectrum Analysis

In the end of the previous chapter, we have highlighted a discrepancy between the collector simulation and the measurements. In particular, there is a gap for the 3rd and 4th stage: the simulated current collected by these electrodes is different from the measurement by a dozen mA. We will determine the root cause and suggest ways to improve the collector simulation.

3.1 Possible Causes

The Collect3D simulation requires several complex input files, like a 3D magnetic field, a 3D mesh and a injection file containing the beam properties (which comes from the interaction computation). Moreover, some parameters of the secondary emission model are adjustable (number of successive emission, emission angles...) to give the user a degree of freedom and to optimize the computation time. However, it could lead to a wrong simulation if the secondary emission parameters are not realistic. Pointing out the root cause of the discrepancy is difficult.

The B-field and the mesh of the collector has been verified and tested, the discrepancy does not come from them. Then, we suspected the secondary emission model. Indeed, the extra 10mA simulated current on C3 (which should be collected by C4 to match the measurement) can come from electrons which get into C4, strike the electrode and give rise to back-scattered or true secondary electrons (see section 2.2.3) which then escape C4 and are collected on C3. This interstage back-flow is a major issue in collector design and precautions are always taken regarding the secondary emissions. To sum up at this point, the two possible causes of the collector simulation are the secondary emission and the particle injection file from MVTRAD.

We focus on the C4 current to determine the root cause. Indeed, as C4 is the last electrode of the collector, there is no backward current into C4 and the electrons that can enter into C4 have the biggest velocity (C4 has the biggest potential of the MDC). The first question we have to answer is: In simulation, do the electrons have enough energy to get into C4 ?

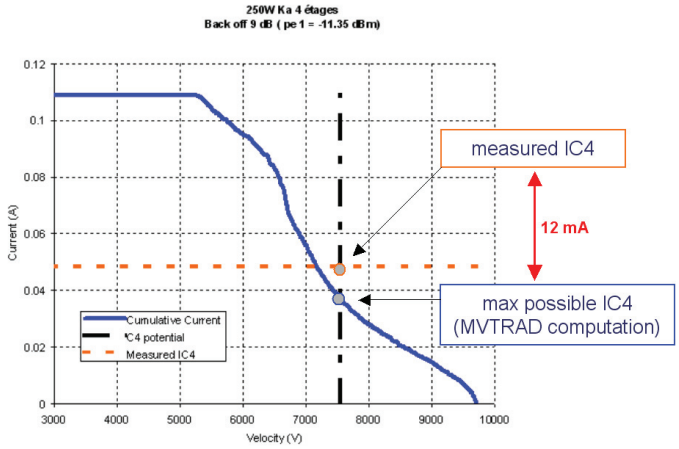

Figure 3.1: Example of velocity spectrum compared to a C4 measurement point.

3.2 Velocity Analysis

After interaction with the wave, the electrons of the beam have a wide range of velocities. It is described by the velocity spectrum (see section 2.2.2). We will use the velocity spectrum to determine the number of electrons that can enter into C4 and we will compare to the measurements. We will focus on the small signal drive (few dB back off from saturation) as we have the biggest discrepancy in this region. First, we analyze a single back off point (-9 dB) and we will extend the reasoning to all back off points.

3.2.1 An example

Let's take the example in Figure 3.1, it is a simulated velocity spectrum at -9 dB back-off. It is a interaction (MVTRAD) computation at the RF output. As a reminder, the velocity spectrum from MVTRAD (beam properties after interaction) is the injection particle file of the collector simulation. The C4 potential (vertical black dashed line) and the IC4 measured current (horizontal orange dashed line) are plotted as a reference.

The cumulative current to the right of the orange dashed line has enough speed to get into C4 whereas the cumulative current to the left does not have enough speed to get into C4. The current which has just enough energy to enter into C4 is then the intersection between the orange dashed line and the cumulative current: the current which has at least the speed of the C4 potential. It is clearly smaller than the measured C4 current (by a dozen mA). Thus, wa can conclude that the beam we inject in the collector is not correct, there are not enough electron able to enter into C4, that is, there are not enough electrons which have at least the speed UC4 in simulation. Therefore, we can conclude that the root cause of the collector simulation discrepancy is the particle injection file.

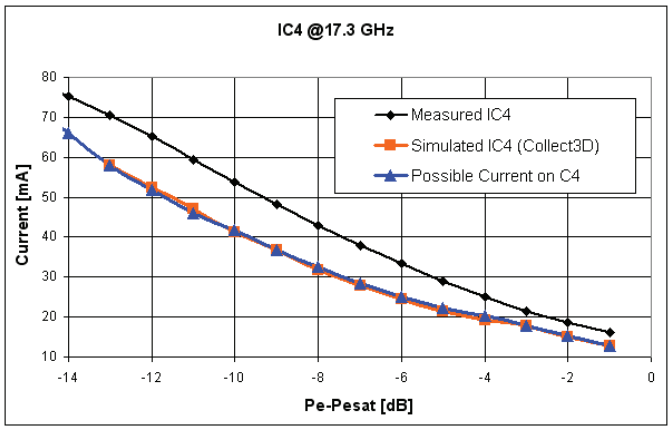

Figure 3.2: Comparaison between the simulated collected current on C4 and the possible current on C4 from the simulated velocity spectrum.

3.2.2 The Root Cause

Moreover, the possible current which can be collected on C4 (estimation based on MVTRAD spectrum i.e. before collector simulation) is smaller than the measurement by a dozen mA, so it is the same difference there is between the simulated current IC4 (after collector simulation) and the measurement. Then, it means that all the current which has enough speed to be collected on C4 is actually collected on C4. This seems trivial but it is not because there could be some backward current escaping C4.

In Figure 3.2, the maximum possible current (blue triangles) than we can get on C4 extracted of the velocity spectrum is compared to the current IC4 after the Collect3D simulation (orange squares) and the measurement (black diamonds). There are two important results to discuss:

1. **simulated IC4 $<$ measured IC4:** In all back-off points of Figure 3.2, the simulated IC4 is smaller than the measured IC4. We saw in the previous example that is it due to the velocity spectrum injected in the collector. What we said for one point (back-off 9dB) is true for all the back-off points: the maximum possible current we could get on the electrode 4 is smaller than the measured current IC4, there are not enough fast electrons, meaning it is impossible to get the good current distribution with this injection file.

2. **Possible current IC4 (before collector computation) = Simulated IC4 (after collector computation):** Despite the discrepancy simulation-measurement, the simulated current IC4 (Collect3D result) corresponds exactly to the possible current IC4 (Collect3D injection). It means that Collect3D computation is correct, in particular, it is a proof that the other input files (the collector mesh and the magnetic field) are correct. Thus, with the correct injection file, we would have a good fit of the collector current distribution.

Then, we want to measure the velocity spectrums at different frequencies and different drives in order to use them as a input file of the collector simulation. Besides, we could compare and quantify the discrepancy with the interaction computation.

3.3 Velocity Measurement

We implement an experiment to measure the velocity spectrum of the beam at the collector input. The principle is straightforward but it is a risky experiment fot the TWT.

3.3.1 Principle

All the electrodes of the collector are set at the same potential UC, as if we had a mono collector. Then, the collector voltage UC is swept from low to high voltage:

- The electrons with a speed bigger than UC are collected on the electrodes giving a collector current IC.
- The electrons with a speed smaller than UC can not enter into the collector, then there are reflected back toward the delay-line, giving an helix current IH.

Thus, at each UC point, we will measure IC and IH. According to the velocity spectrum we have seen earlier, we expect the collector current IC to decrease when increasing UC and the helix current IH to increase when increasing UC.

3.3.2 Risks

A lot of current is expected to strike the helix, especially when we get close to the helix potential (initial speed of the beam). The helix is fragile and too much current breaks it because of the too high temperature. Drastic precautions are usually taken regarding the helix current IH and specifications limits it. Though, our experiment requires a high IH to describe the velocity spectrum. So, we have to work with a current modulator.

3.3.3 Setup

We use a very low duty (0.01 %) at a frequency modulation of 50 Hz. It means that every 20ms, the current is ON for $2\mu s$ and OFF for the rest of the period. Thus, the helix current is high but for a very short time, so there is no danger for the TWT's life. We use current coils to measure the current, high voltage and RF probes to measure the voltage and we observe the result on an oscilloscope. We measure the collector current IC and the helix current IH as shown in Figure 3.3.

We see that the sum of the current is constant, IC and IH courterbalance each other, so the experiment is a success. UC describes then the velocity spectrum. Now, we want to inject the measurement of the velocity spectrum of the beam in the collector.

3.4 Injection File

The measurement of the velocity spectrum is used as the particle injection file of the collector. However, it needs to be adapted because the measurement is not accurate enough.

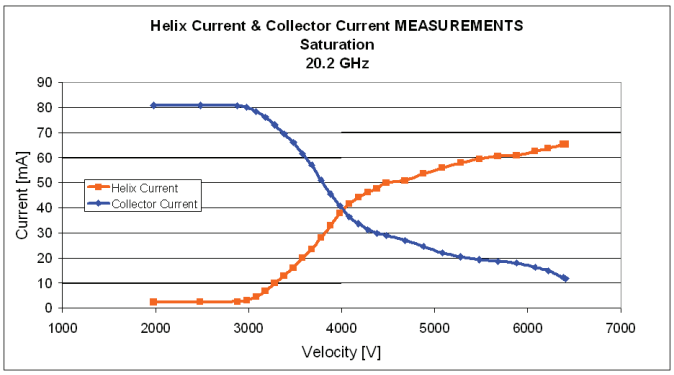

Figure 3.3: Measurement of IC and IH.

3.4.1 Description

The injection file contains the position and the velocity of each particle in three directions. From the measurement, we get no information about the radial and azimutal position and we measure only the module of the velocity. In fact, we have to build a vector having only the modulus.

3.4.2 Assumption

The axial velocity is several order bigger than the radial and azimutal velocity, so we will assume that the descrepancy in velocity modulus between the measurement and the simulation is only due to the axial velocity. We also assume that the simulated velocity spectrum is not too far from reality and we keep steady the radial and azimutal velocity.

3.4.3 Modification of the injection file

Under the assumption that the axial velocity is dominant, we only change the axial velocity of the simulated spectrum. Actually, we modify it to make the velocity module match the velocity measurements. Thus, we have written a python code that change the simulated velocity in order to intersect points defined by the user (those points are chosen to match the measurement basically). In Figure 3.4, an example of a spectrum modification is presented, the maximum possible current is increased.

The code contains three steps as shown in Figure 3.5. First, we compute the velocity module and plot the velocity spectrum from the injection file. Then, we define a target point the curve must intersect. The easiest idea to make the curve intersect this point is to translate it. Finally, after the translation in Volts, we reset the initial min and max velocities - or we can set new ones - and the injection file is rewritten with the assumption that only the axial velocity changes.

3.5 Prospects

So far, we have shown that we are able to measure the velocity spectrum with success. Working under unusual conditions (mono-collector), the power supply requires a good current modulator and

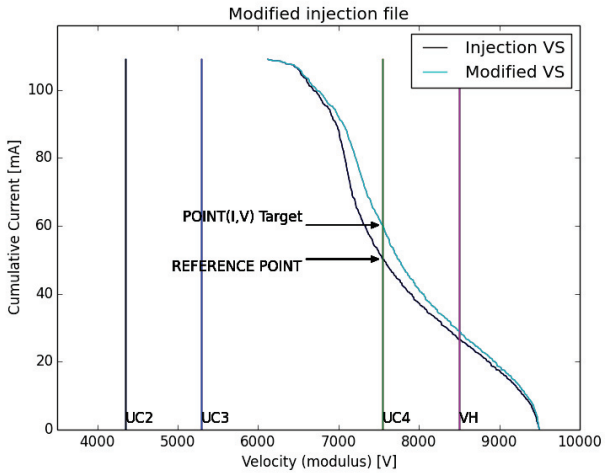

Figure 3.4: Modification of the Velocity Spectrum with the code.

attention has to be paid regarding the regulation of the power supply. Moreover, to be able to make comparaison between different TWTs, the phase-shift and the interaction efficiency of the TWTs have to be measured at each drive modes. The expriment has been approved but measurements do not have been done on the 250 W Ka TWT yet. When the measurements is done, we will compare them to the simulation and change the simulated spectrum according to the measurement with the python code. We will do collector simulation with the new velocity spectrum, meaning with new injection files and we expect a good fit of the current distribution.

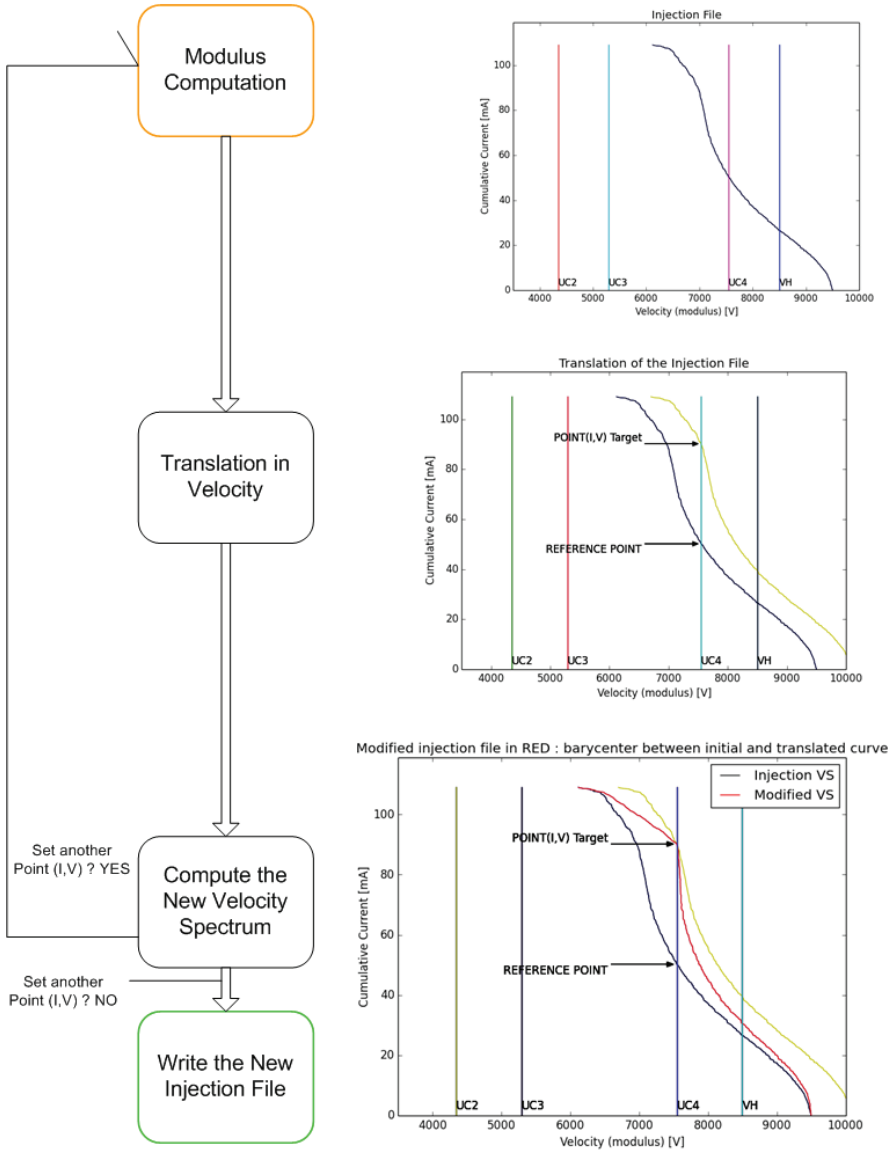

Figure 3.5: Description and illustration of the code.

Conclusion

The global objective of the internship was to improve the electric efficiency of a 250W Ka space TWT. It is divided in two steps: the fit of the existing 4-stages collector and the optimization of the collector by adding a 5th stage. At the end of the first part, after the 4-stages collector simulation, a large discrepancy between the simulation and the measurements has been observed. In particular, the estimated current distribution on the four electrodes of the collector do not fit. The root cause lies in the electron beam velocity spectrum, the simulation gving a beam slower than the measurements. The velocity spread is a consequence of the interaction (the electrons give their kinetic energy to amplify the wave). That means a little divergence in the interaction modelization results in a wrong in velocity spectrum that leads to a divergence in current distribution of the collector. The issue has not been solved yet, the conception of a new collector with a higher electric efficiency could not be done. However, the root cause of the discrepancy in collector simulation has been highlighted and the simulation process has been reconsidered with a fresh look. First, the computations has been chained to improve the global computation time. Then, we pay a lot more attention to the velocity spectrum we inject in the collector, in particular, we have made velocities measurements and created a tool to change the velocity spectrum in order to understand accurately its influence on the collector current distribution.

To go further, measurements have to be done on the TWTs of interest while paying a particular attention to the phase shift and the interaction efficiency to be able to compare TWTs of the same range. Indeed, due to the production gap, two TWTs with the same design can have different performances. Then, the velocity experiment should be simulated with collect3D. The TWT does not work in normal conditions in this experiment (all electrodes of the collector at the same potential), so it is interesting to analyze simulations in this particular mode. Finally, after drawing comparisons between measured and simulated velocity spectrum, we will adapt the simulated spectrum to the measurements. The idea is to create a set of injection file for the collector at different frequencies and different drives. After what we will be able to retrosimulate the TWT and optimize the performances of the collector. Having the good input files, the optimization of the new collector will be more accurate, quicker and simplified.

References

1. Gilmour, A.S. Jr. Microwaves Tubes, ch. 10.2 Traveling Wave Interaction, USA, Artech House, 1986.

2. Brewer G., "Focusing of high-density electron beams"', « Focusing of charged particles », Spetier A, USA, Academic press, 1967

3. Durand, E. Magnétostatique,ch. X - Aimants Permanents, Paris, Masson et Cie, 1968.

4. Plouin, Juliette. "Injection d'Harmonique dans un Tube à Ondes Progressives : Amélioration de la Puissance de Sortie", Paris, Ph.D Thesis, Ecole Polytechnique, 2010.

5. Okoshi, Takanori. The Tilted Electric Field Soft-Landing Collector and Its Application to a Traveling-Wave Tube, IEEE TRANSACTIONS ON ELECTRON DEVICES, VOL. ED-1.9, YO. 1, JANTJARY 1972.

6. Valfells, Agust. Advancements in Codes for Computer Aided Design of Depressed Collectors and Tracing of Backscattered Electrons Part II: Improvements in Modeling of the Physics of Secondary Electron Emission and Backscattering, IEEE TRANSACTIONS ON PLASMA SCIENCE, VOL. 30, NO. 3, JUNE 2002.

7. Kosmahl, Henry G. How to Quickly Predict the Overall TWT and the Multistage Depressed Collector Efficiency, IEEE TRANSACTIONS ON ELECTRON DEVICES, VOL. ED-27, NO. 3, MARCH 1980, p.526.

8. Dayton, James A. Analytical Prediction and Experimental Verification of TWT and Depressed Collector Performance Using Multidimensional Computer Programs, IEEE TRANSACTIONS ON ELECTRON DEVICES, VOL. ED-26, NO. 10, OCTOBER 1979, p.1589.

9. Bernadi, Pierre. "Utilisation et AmÍioration du Modèle Discret d'Excitation d'un Guide d'Onde Périodique pour la Simulation Pratique du Tube à Onde Progressive en Domaine Temporel", Vélizy, Ph.D Thesis, Université de Provence, 2011.

Series of Master's theses
Department of Electrical and Information Technology
LU/LTH-EIT 2015-469

http://www.eit.lth.se